An Improved De-Embedding Technique for the Measurement of the Complex Constitutive Parameters of Materials Using a Stripline Field Applicator

George W. Hanson, *Member, IEEE*, Jerry M. Grimm, *Member, IEEE*, and Dennis P. Nyquist, *Member, IEEE*

***Abstract*—A method for measuring the electromagnetic constitutive parameters of materials using a strip transmission-line field applicator is presented. A technique is developed to measure the scattering parameters of the imperfect transition regions between the applicator coaxial terminal ports and the front and back terminal planes of the material sample in stripline. *S*-parameters of the sample region are subsequently de-embedded from the coaxial-terminal *S*-parameters using the measured transition-region network model. The complex permittivity and permeability of the sample are easily related to the sample's *S*-parameters through well known analytic relations. Measured constitutive parameters are presented for several representative materials.**

I. Introduction

THIS paper presents a method for the measurement of complex permittivity and permeability of a material sample embedded in a strip transmission line. Transmission line field applicators are often used for the measurement of material properties in both time and frequency domains [1]–[9]. The general frequency-domain method was described by Weir [2] using a rectangular waveguide. Coaxial and stripline systems are also common, and broad-band measurements are typically made with an automatic network analyzer (ANA). The measurement technique, generally referred to as the transmission/reflection (T/R) method, involves measuring the complex transmission and reflection coefficients (*S*-parameters) of the material sample, leading to determination of the desired material parameters.

The strip transmission line provides a flexible material measurement system. Material samples can be inserted above and below the center strip through the open sides between the ground planes, and the stripline geometry requires only relatively simple machining of the sample. The stripline is a broad-band field applicator, propagating TEM waves with essentially unidirectional electric and magnetic fields. Anisotropic effects can be inferred by rotating the sample, which is an advantage over the coaxial transmission-line field applicator. In addition, there is no cutoff frequency as encountered in waveguide systems. Coaxial and waveguide systems do have the advantage that precision calibration standards are available, and accurate calibration of the ANA to the sample's reference planes may be performed.

The purpose of this paper is to demonstrate a T/R measurement technique using the *S*-parameters of a material sample which are de-embedded from the measured terminal *S*-parameters of a transmission-line field applicator. The *S*-parameters of the imperfect transition regions between coaxial terminal ports and the front and back terminal planes of the sample region are found using only short circuits. *S*-parameters of the sample region are subsequently de-embedded from the coaxial-terminal *S*-parameters using the measured transition-region network model. This leads to substantially improved accuracy in determining the sample's *S*-parameters, resulting in enhanced accuracy of the complex permittivity ϵ_r and permeability μ_r. Results are presented for measurements made in a stripline field applicator, although the de-embedding method is applicable to a variety of transmission line systems, including microstrip [10].

The organization of this paper is as follows. Section II-A provides an *S*-parameter description of a transmission line transition, and the potential inaccuracy of simple phase-shift correction is discussed. In Section II-B, equations are derived which relate the desired sample-region *S*-parameters to the unknown *S*-parameters of the transition regions. In Section II-C, a method is developed to determine the transition region *S*-parameters. Section III describes the transmission line field applicator and measurement procedure, followed by measured results and conclusions.

II. Theory

A transmission line system for the measurement of relative permittivity ϵ_r and relative permeability μ_r is depicted in Fig. 1(a). The unknown sample of finite thickness is inserted into the transmission line, creating a discontinuity within the line. Swept frequency measurements are made with an ANA at terminal planes A and B.

Manuscript received April 27, 1992; revised September 29, 1992.

G. W. Hanson is with the Department of Electrical Engineering and Computer Science, the University of Wisconsin at Milwaukee, Milwaukee, WI 53201.

D. P. Nyquist is with the Department of Electrical Engineering, Michigan State University, East Lansing, MI 48823.

J. M. Grimm is with the Center for Naval Analyses, Alexandria, VA 22302-0268.

IEEE Log Number 9207678.

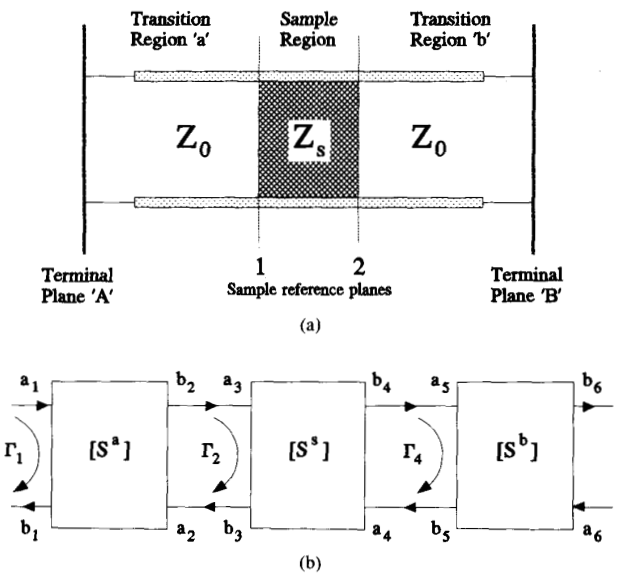

Fig. 1. (a) Transmission-line field applicator with sample inserted. (b) Equivalent two-port network.

Transition region 'a' is that portion of the transmission line from the coaxial terminal plane A to the sample front reference plane 1. Similarly, transition region 'b' is that portion of the measurement system from the sample back reference plane 2 to coaxial terminal plane B. Both transition regions are air-filled and isotropic. The *S*-parameter network model for this system is given in Fig. 1(b). In this representation, $[S^a]$ models transition region 'a,' $[S^s]$ models the sample region, and $[S^b]$ models transition region 'b.'

The determination of ϵ_r and μ_r involves the simultaneous solution of

$$\beta(\omega, \mu, \epsilon) - \beta_m(\omega) = 0$$

$$\Gamma(\omega, \mu, \epsilon) - \Gamma_m(\omega) = 0 \tag{1}$$

where β is the propagation constant of the sample-loaded section of the transmission line, and Γ is the interfacial reflection coefficient associated with the front of that region, with β_m and Γ_m being the measured quantities. This is a pair of nonlinear equations in two unknowns, the solution of which is seen to decompose into two parts. First, an analytical theory is needed to relate $\beta(\omega, \mu, \epsilon)$ and $\Gamma(\omega, \mu, \epsilon)$ to the complex constitutive parameters ϵ_r and μ_r. This requirement is easily met by using stripline in the TEM mode, as $\beta = \omega\sqrt{\mu\epsilon}$ and Γ is defined in terms of easily developed characteristic impedances. Second, a technique to accurately measure β_m and Γ_m is required. The technique used here is that of Nicolson and Ross [1] and Weir [2] (referred to as NRW), summarized in the appendix, which makes use of the measured scattering parameters of the sample, $[S^s]$, to determine β_m and Γ_m. For accurate results, the sample *S*-parameters must be measured carefully. The focus of this paper is the careful extraction or the sample region *S*-parameters from measurements, and their subsequent use in the NRW equations.

A. S-Parameter Description of Transition Region

To implement the NRW technique, the calibration planes for the sample's *S*-parameters are assumed to be the front and back sample planes. In general, the ANA cannot be calibrated to the front and back reference planes of the sample, since these locations are not accessible to measurement. Even if the sample reference planes could be made available, precision loads needed for calibration may not exist, as in the case of stripline or microstrip. A simple method to transform the terminal plane *S*-parameters to the front and back sample reference planes is to account for the phase delay through the transition regions (phase-shift correction). This is easily seen to be inadequate unless the transitions from the ANA coaxial system to the transmission line system are nearly perfect, as illustrated below.

Referring to the signal flow graph Fig. 1(b), the reflection coefficient seen at port 1, Γ_1, is given as

$$\Gamma_1 = S_{11}^a + \frac{S_{21}^a S_{12}^a \Gamma_2}{1 - \Gamma_2 S_{22}^a} \tag{2}$$

while the signal seen at the output of region 'a' is

$$b_2 = \frac{S_{21}^a}{1 - \Gamma_2 S_{22}^a} a_1. \tag{3}$$

With this model for the input transition-region 'a,' the need for a good impedance match is clearly seen. With a shorting plate located at the sample's front interface 1 ($\Gamma_2 = -1e^{-j0}$), the reflection coefficient measured at the transmission line terminal plane A due to transition region 'a' is

$$\Gamma_1 = S_{11}^a - \frac{S_{12}^a S_{21}^a}{1 + S_{22}^a} \tag{4}$$

Under the assumption that $S_{11}^a = 0$ and $S_{22}^a = 0$, phase information from the measured reflection coefficient determines the transition-region electrical length, which is used to translate the measured coaxial-terminal plane *S*-parameters to the *S*-parameters of the sample region. It is clear that the occurrence of $S_{11}^a \neq 0$ or $S_{22}^a \neq 0$ degrades the determination of the transition-region electrical length, and leads to errors in the de-embedded *S*-parameters of the sample. In an alternative procedure, the total transmission coefficient S_{21}^t of the empty stripline may be measured, and the desired shift factor determined by subtracting the physical length of the sample from the measured electrical length and dividing by two [6], assuming the sample is placed in the stripline center. For this procedure to be accurate, all the reflection *S*-parameters of transition regions 'a' and 'b' must be zero, or $S_{11}^a = S_{22}^a = S_{11}^b = S_{22}^b = 0$. It has been found that although $S_{11}^{a,b}$, $S_{22}^{a,b}$ are small for a well designed stripline (< -25 dB typ.), significant improvement of measured results can be achieved by correctly accounting for the impedance mismatch of the transition regions. Correcting for the impedance mismatch also allows for added flexibility to accommodate samples of varying sizes. Usually, the

transmission line system is designed for the minimum reflections, and the material sample is cut and machined to fit snugly into the transmission line. Once the system is designed, there is no flexibility as to what size sample may be measured. With the method described here, good matching between the transmission line and the ANA coaxial cables is not critical. For the case of the stripline system, the spacing of the ground planes can be adjusted to accommodate the sample, and rectangular samples of nonsquare cross section can be rotated to measure the material parameters in any specific direction.

B. De-Embedding of Sample Scattering Parameters

Referring to the two-part network model described by Fig. 1(b), the forward measured terminal S-parameters at terminal plane A, S_{11}^t and S_{21}^t, can be formulated as

$$\Gamma_1^t = S_{11}^a + \frac{(S_{21}^a)^2 \Gamma_2}{1 - \Gamma_2 S_{22}^a} \tag{5}$$

$$S_{21}^t = \frac{S_{21}^a}{1 - \Gamma_2 S_{22}^a} \frac{S_{21}^s}{1 - \Gamma_4 S_{22}^s} S_{21}^b \tag{6}$$

where $\Gamma_1^t = S_{11}^t$ for a match termination at port 6 (terminal plane B). Γ_2 and Γ_4 are the reflection coefficients at port 2 and port 4, respectively, and the isotropic behavior of the air-filled transition regions ($S_{12}^a = S_{21}^a$) has been taken into account. The reflection coefficient at port 4, Γ_4, has the same form as (2); however, no reflection is seen at port 6 ($\Gamma_6 = 0$) if match is terminated, and thus Γ_4 becomes

$$\Gamma_4 = S_{11}^b. \tag{7}$$

The reflection coefficient Γ_2 at port 2 also has the same form as (2), namely,

$$\Gamma_2 = S_{11}^s + \frac{S_{21}^s S_{12}^s \Gamma_4}{1 - \Gamma_4 S_{22}^s} \tag{8}$$

and includes the effects of *both* the sample region and transition region 'b' (through Γ_4). Reflection coefficient Γ_2 is also the total reflection coefficient seen at the front sample interface, and not just the interfacial reflection coefficient.

Both (6) and (8) are in terms of all the sample S-parameters, providing a simultaneous set of two equations in four unknowns. But under the assumptions inherent in developing the formulas in the appendix, the sample in question is symmetric, thus $S_{11}^s = S_{22}^s$ and $S_{21}^s = S_{12}^s$. Equations (6) and (8) become

$$\frac{S_{21}^s}{1 - S_{11}^b S_{11}^s} = Q = S_{21}^t \frac{(1 - \Gamma_2 S_{22}^a)}{S_{21}^a S_{21}^b}$$

$$S_{11}^s + \frac{(S_{21}^s)^2 S_{11}^b}{1 - S_{11}^b S_{11}^s} = P = \Gamma_2 \tag{9}$$

where Γ_2 is determined from (5) as

$$\Gamma_2 = \frac{\Gamma_1^t - S_{11}^a}{(\Gamma_1^t - S_{11}^a) S_{22}^a + (S_{21}^a)^2}. \tag{10}$$

Equation pair (9) is in terms of only two unknown sample S-parameters, S_{11}^s and S_{21}^s, and can be solved to yield.

$$S_{11}^s = \frac{P - S_{11}^b Q^2}{1 - (S_{11}^b Q)^2}; \quad S_{21}^s = \frac{Q(1 - S_{11}^b P)}{1 - (S_{11}^b Q)^2} \tag{11}$$

where P and Q are coefficients depending upon the measured data, defined in (9) and (10) as

$$P = \frac{\Gamma_1^t - S_{11}^a}{(\Gamma_1^t - S_{11}^a) S_{22}^a + (S_{21}^a)^2}; \quad Q = S_{21}^t \frac{(1 - \Gamma_2 S_{22}^a)}{S_{21}^a S_{21}^b}. \tag{12}$$

The relations (11) and (12) provide a method for the desired sample S-parameters to be de-embedded from the measured terminal plane S-parameters.

C. Characterization of Field Applicator Transition Regions

The de-embedding formulas (11) cannot be utilized unless the coefficients in (12) can be computed; to accomplish this the transition region parameters S_{11}^a, $(S_{21}^a)^2$, S_{22}^a, S_{11}^b, and $S_{21}^a S_{21}^b$ are needed. These can be found by making additional terminal S-parameter measurements.

Recall that (5) relates the measured reflection coefficient at reference plane A to the reflection coefficient at the sample's front interface in terms of S_{11}^a, S_{22}^a, $S_{12}^a S_{21}^a$, three currently unknown S-parameter *quantities* in terms of transition region 'a' S-parameters. Measurements of the reflection coefficients for three known loads at the sample front interface allow a determination of the three unknown S-parameters quantities in terms of the measured and known load reflection coefficients. A typical set of loads would be a short ($\Gamma = -1$), an open ($\Gamma = +1$), and a precision matched termination ($\Gamma = 0$); stripline presents an interesting challenge since the sample reference plane is inaccessible, except for being able to insert a shorting bar. The key to actually characterizing transition region 'a' is to use three different locations of the shorting bar within the applicator, which will result in three unique, known reflection coefficients to provide calibration standards. In this case, the shorting bars will provide the calibration reflection coefficient

$$\Gamma_2^{ci} = -1\, e^{-j2k_o d_i} \cdots i = 1, 2, 3 \tag{13}$$

where d_i is an axial shift from the physical location of sample front interface. For convenience, the shifts $d_1 = 0$, $d_2 = +\ell$, $d_3 = -\ell$ were used. The value of ℓ was typically chosen as $\lambda/10$, with λ the wavelength at the middle of the frequency range of interest. This calibration scheme, in conjunction with (5), determines the following quantities:

$$K^c = \frac{(\Gamma_1^{c3} - \Gamma_1^{c1})}{(\Gamma_1^{c2} - \Gamma_1^{c1})} \frac{(\Gamma_2^{c2} - \Gamma_2^{c1})}{(\Gamma_2^{c3} - \Gamma_2^{c1})} \tag{14}$$

$$S_{22}^a = \frac{K^c - 1}{K^c \Gamma_2^{c3} - \Gamma_2^{c2}} \tag{15}$$

$$(S_{21}^a)^2 = (\Gamma_1^{c2} - \Gamma_1^{c1}) \frac{(1 - S_{22}^a \Gamma_2^{c1})(1 - S_{22}^a \Gamma_2^{c2})}{(\Gamma_2^{c2} - \Gamma_2^{c1})} \quad (16)$$

$$S_{11}^a = \Gamma_1^{c1} - \frac{S_{12}^a S_{21}^a \Gamma_2^{c1}}{1 - S_{22}^a \Gamma_2^{c1}}. \quad (17)$$

Two observations are appropriate here. First, if any of the calibration shorts are a half-wavelength apart ($\ell = n\lambda/2$), then $\Gamma_2^{c2} = \Gamma_2^{c3}$, and calibration constant $K^c = 1$, making S_{22}^a an indeterminate quantity. At this point, the calibration scheme is unstable. Second, observe that $(S_{21}^a)^2$ is determined, not S_{21}^a. Determining S_{21}^a involves taking a square root, which introduces a sign ambiguity. Some other criterion or measurement is necessary to resolve the ambiguity, making this operation undesirable. While knowledge of S_{21}^a is necessary to fully characterize transition region 'a,' it is seen by (12) that determination of $(S_{21}^a)^2$ provides sufficient information for de-embedding purposes, if the product $S_{21}^a S_{21}^b$ can be determined. Also, the remaining transition region 'b' S-parameters could be obtained by a similar process, although S_{22}^b is not needed, and determining S_{21}^b introduces the same problems as mentioned previously.

A procedure to bypass determining the square root for either S_{21}^a or S_{21}^b is to make empty applicator measurements. In this situation, the sample region is assumed to be air-filled, and the air-filled sample S-parameters are known to be

$$S_{11}^s = 0; \quad S_{21}^s = e^{-jk_0 l_s} \quad (18)$$

where l_s is the sample length. If the forward S-parameters of the applicator are measured, then

$$S_{21}^e = \frac{S_{21}^a S_{21}^b e^{-jk_0 l_s}}{1 - \Gamma_2^e S_{22}^a}; \quad \Gamma_2^e = S_{11}^b e^{-j2k_0 l_s} \quad (19)$$

where Γ_2^e is defined in (10), using Γ_1^e in place of Γ_1^t. As becomes clear from (19), the needed transition region 'b' S-parameters are determined as

$$S_{11}^b = \Gamma_2^e e^{+j2k_0 l_s} \quad (20)$$

$$S_{21}^a S_{21}^b = S_{21}^e (1 - \Gamma_2^e S_{22}^a) e^{+jk_0 l_s}. \quad (21)$$

Observe that only the product $S_{21}^a S_{21}^b$ is determined, although, as observed earlier, this is sufficient for the S-parameter de-embedding.

III. Field Applicator Design and Measurement Procedure

The goal of this research was to measure the electromagnetic constitutive parameters of materials which may be considered as large-scale homogeneous and/or anisotropic, in the frequency range 100–2000 MHz. This measurement requires the interrogation of large field volumes by a field applicator which maintains an essentially TEM wave. Consequently, a stripline field applicator was constructed for the measurement of complex permittivity and permeability. The top and side views of the stripline are shown in Fig. 2 for one end of the stripline; and the other end is identical. The dimensions of the stripline applicator are: total length = 1 m, ground plane width = 25.4 cm, center conductor width = 10 cm, and center conductor thickness = 0.16 cm. In order to provide a good impedance match, the center conductor was tapered (18° with respect to the endplate), and tapered corners were inserted at the two ends of each ground plane to form tuning wedges. The ground planes and tapered corners are allowed to move vertically along slots cut in the endplates. This was initially done to determine the proper ground plane spacing (7.5 cm) to obtain a good impedance match for the empty stripline. With the utilization of the de-embedding technique, impedance matching is not critical, and the ground planes were allowed to move to accommodate samples of different size.

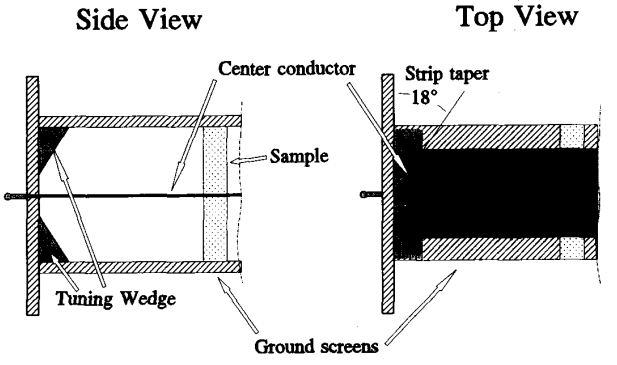

Fig. 2. Stripline field applicator.

The measurement procedure may be divided into four steps as outlined below:

1) Calibrate the ANA, assumed to have coaxial cables, to the terminal reference planes A and B. All measurements were made with an HP 8720B, using the standard 2-port, 12-term error correction calibration.
2) Measure the S-parameters of the imperfect transition regions "a" and "b," by using three different short circuit measurements and the two forward S-parameter measurements of the empty applicator. The necessary S-parameters are calculated using (14)–(17) and (20)–(21).
3) Measure the forward S-parameters at the stripline terminal planes A and B. The sample region S-parameters are de-embedded from the terminal plane measurements by (11) and (12), using the measured transition-region model from Step 2.
4) Compute the material parameters ϵ_r and μ_r from the de-embedded sample S-parameters by the NRW method detailed in the appendix, using (A.2) and (A.3)

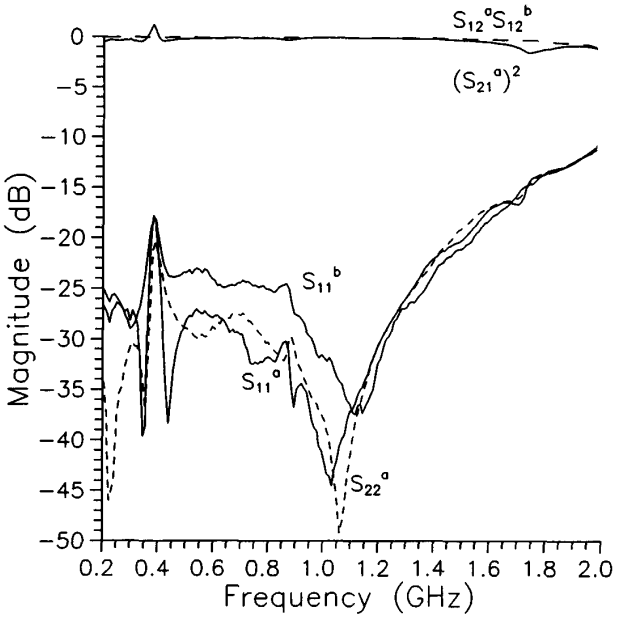

Fig. 3. Magnitude of computed S-parameters for transition regions.

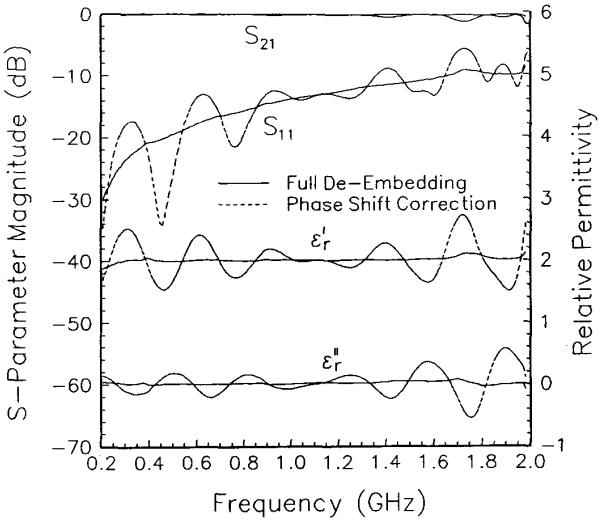

Fig. 4. Comparison of measured S-parameters and material parameters of a Teflon sample obtained by phase shift correction and de-embedding.

IV. Measured Results

The stripline applicator described above was constructed, and its transition region models were calculated by the technique described in this paper. Fig. 3 shows the computed S-parameters for the two transition regions. It is seen that $(S_{21}^a)^2$ corresponds to a virtually lossless section of transmission line, and the magnitudes of S_{11}^a and S_{22}^a are less than -25 dB over more than half of the band, although increasing at the higher frequencies. A low-reflection parameter indicates a well designed coax-to-stripline transition, as S_{11}^a is a direct measurement of the reflection from the coax-to-stripline transition at port 1. The magnitudes of $S_{21}^a S_{21}^b$ and S_{11}^b behave as expected for a relatively well-matched transmission system. The magnitudes of S_{11}^b and S_{22}^a are very similar, since they represent the same type of coax-to-stripline transition, one at each end of the stripline.

Fig. 4 presents a comparison between S-parameters (11) and material parameters (A.3) of a material sample found by de-embedding, and those determined by simple phase-shift correction. In this figure, the sample is Teflon (ϵ_r = 2.05). It is apparent that even with minimal reflections from the coax-to-stripline transition, there is a dramatic effect on the measured magnitudes of the S-parameters. Fig. 5 shows the measured complex permittivity and permeability for both Plexiglas (ϵ_r = 2.5) and Teflon samples, obtained by de-embedding. These samples were of different thicknesses, and neither sample was a half-wavelength long in the frequency range for the measurements. Agreement with known results is good.

As a final test of the de-embedding method, an intentional mismatch was introduced at one transition region

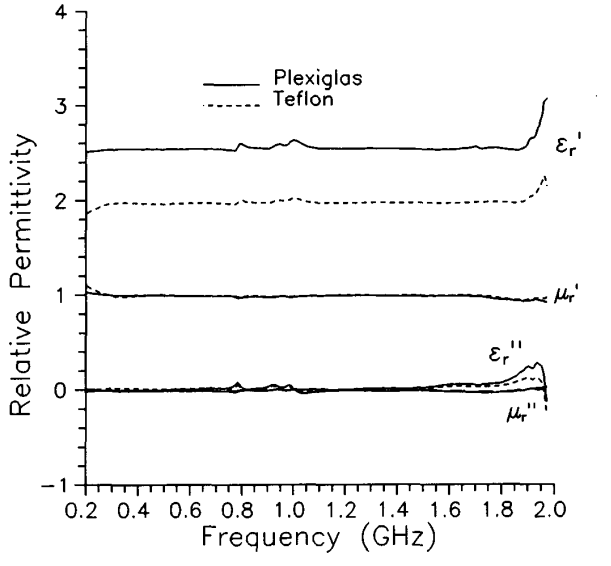

Fig. 5. Measured constitutive parameters for Teflon (ϵ_r' = 2.05, μ_r' = 1.0) and Plexiglas (ϵ_r' = 2.5, μ_r' = 1.0).

port by using a 50 Ω feed-through in cascade with the coaxial stripline terminals. The stripline configuration was the same as in Fig. 3 ($\approx$50 Ω), and so the 50 Ω feed-through created an effective 25 Ω impedance. In Fig. 6, measurements of Teflon's ϵ_r are presented for both the de-embedding technique and the phase-shift correction technique, with and without the intentional mismatch. As becomes quite obvious when the transition region match is poor, the phase-shift correction technique breaks down completely, while the de-embedding technique still returns correct results.

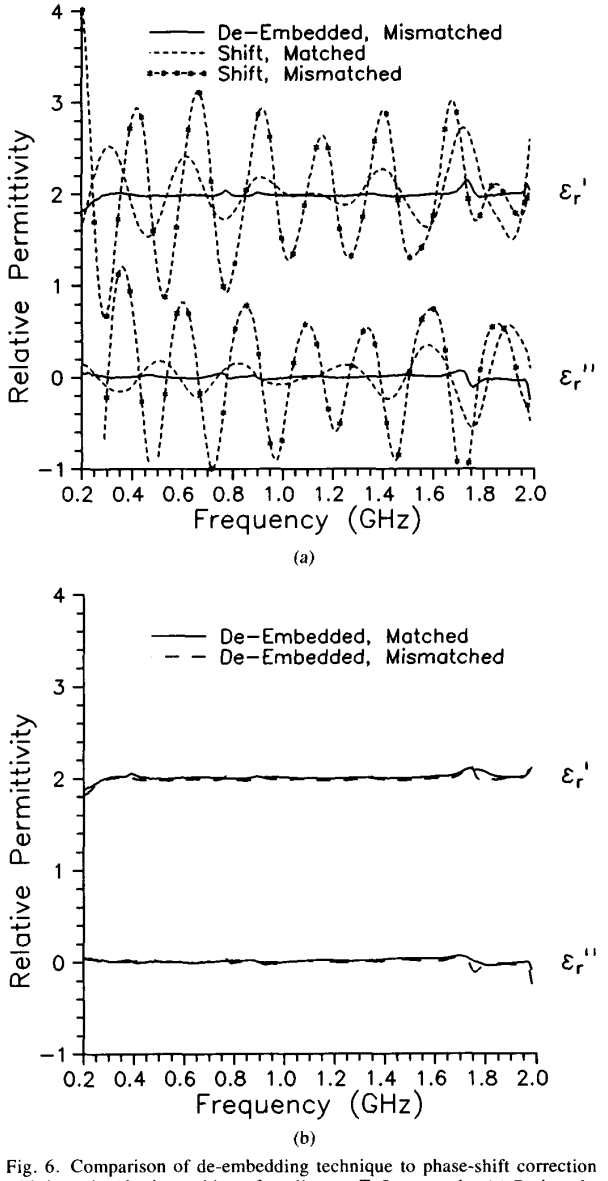

Fig. 6. Comparison of de-embedding technique to phase-shift correction with intentional mismatching of applicator, Teflon sample. (a) Both techniques for matched and mismatched applicator. (b) De-embedding only, both matched and mismatched applicator.

V. Conclusions

A method for determining the electromagnetic constitutive parameters ϵ_r and μ_r from a sample embedded in a strip transmission line is presented. This method accounts for the imperfect transition regions between the stripline's coaxial terminal ports and the sample region's front and back reference planes, resulting in improved computation of permittivity ϵ_r and permeability μ_r. Results are presented which demonstrate the effectiveness of this method, and measurements of several representative materials are included.

Appendix

The Nicholson-Ross-Weir[1] (NRW) T/R technique is utilized in this analysis to obtain β and Γ from the measured sample scattering parameters. A summary of the results is presented here, with details available in [1] and [2]. The S-parameters of the sample region are:

$$S_{11}^s = \frac{\Gamma(1 - z^2)}{1 - (\Gamma z)^2}; \quad S_{21}^s = \frac{z(1 - \Gamma^2)}{1 - (\Gamma z)^2} \tag{A.1}$$

with propagation factor $z = \exp(-j\beta l)$ and interfacial reflection coefficient

$$\Gamma = \frac{Z_s - Z_0}{Z_s + Z_0}.$$

It is possible to solve (A.1) for z and Γ, with the results

$$\Gamma = K \pm \sqrt{K^2 - 1}; \quad z = \frac{(S_{11}^s + S_{21}^s) - \Gamma}{1 - \Gamma(S_{11}^s + S_{21}^s)}$$

$$K = \frac{1 + (S_{11}^s + S_{21}^s)(S_{11}^s - S_{21}^s)}{2S_{11}^s}. \tag{A.2}$$

Using the relations in (A.2) with the definitions of β and Γ subsequently leads to the determination of ϵ_r and μ_r. Explicitly, for the TEM stripline,

$$\epsilon_r = \frac{\beta}{k_0}\left(\frac{1 - \Gamma}{1 + \Gamma}\right) \quad \mu_r = \frac{\beta}{k_0}\left(\frac{1 + \Gamma}{1 - \Gamma}\right). \tag{A.3}$$

References

[1] A. M. Nicolson and G. F. Ross, "Measurement of the intrinsic properties of materials by time-domain techniques," *IEEE Trans. Instrum. Meas.*, vol. IM-19, pp. 377–382, Nov. 1970.

[2] W. B. Weir, "Automatic measurement of complex dielectric constant and permeability at microwave frequencies," *Proc. IEEE*, vol. 62, pp. 33–36, Jan. 1974.

[3] S. S. Stuchly and M. Matuszewski, "A combined total reflection-transmission method in application to dielectric spectroscopy," *IEEE Trans. Instrum. Meas.*, vol. IM-27, pp. 285–288, Sept. 1978.

[4] L. P. Ligthart, "A fast computational technique for accurate permittivity determination using transmission line methods," *IEEE Trans. Microwave Theory Tech.*, vol. MTT-31, pp. 249–254, March 1983.

[5] J. Ness, "Broad-band permittivity measurements using the semi-automatic network analyzer," *IEEE Trans. Microwave Theory Tech.*, vol. MTT-33, pp. 1222–1226, Nov. 1985.

[6] W. Barry, "A broad-band, automated, stripline technique for the simultaneous measurement of complex permittivity and permeability," *IEEE Trans. Microwave Theory Tech.*, vol. MTT-34, pp. 80–84, Jan. 1986.

[7] N. Belhadj-Tahar, A. Fourrier-Lamer, and H. De Chanterac, "Broad-band simultaneous measurement of complex permittivity and permeability using a coaxial discontinuity," *IEEE Trans. Microwave Theory Tech.*, vol. 38, pp. 1–7, Jan. 1990.

[8] J. Baker-Jarvis, E. J. Vanzura, and W. A. Kissick, "Improved technique for determining complex permittivity with the transmission/reflection method," *IEEE Trans. Microwave Theory Tech.*, vol. 38, pp. 1096–1103, Aug. 1990.

[9] K. M. Fidanboylu, S. M. Riad, and A. Elshabini-Riad, "A new time-domain approach for determining the complex permittivity using stripline geometry," *IEEE Trans. Instrum. Meas.*, vol. 39, pp. 940–944, Dec. 1990.

[10] G. W. Hanson, D. P. Nyquist, B. Kzadri, J. Grimm, M. Thorland, and L. Frasch, "Electromagnetic Characterization of Materials Using Stripline/Microstrip Field Applicator," in *Natl. Radio Science (USNC/URSI) Meeting*, Univ. of Colorado, Boulder, CO, *Digest* Jan. 1992, p. 279.

[1]This terminology courtesy of Baker-Jarvis at NIST [8].